

Semi-Supervised Learning Approach for Efficient Resource Allocation with Network Slicing in O-RAN

Salar Nouri[†] Mojdeh Karbalaee Motalleb[†] Vahid Shah-Mansouri[†] Seyed Pooya Shariatpanahi[†]

[†] School of Electrical and Computer Engineering, College of Engineering, University of Tehran, Tehran, Iran
 {salar.nouri, mojdeh.karbalaee, vmansouri, p.shariatpanahi}@ut.ac.ir

Abstract—This paper introduces an innovative approach to the resource allocation problem, aiming to coordinate multiple independent x-applications (xAPPs) for network slicing and resource allocation in the Open Radio Access Network (O-RAN). Our approach maximizes the weighted throughput among user equipment (UE) and allocates physical resource blocks (PRBs). We prioritize two service types: enhanced Mobile Broadband and Ultra-Reliable Low-Latency Communication. Two xAPPs have been designed to achieve this: a power control xAPP for each UE and a PRB allocation xAPP. The method consists of a two-part training phase. The first part uses supervised learning with a Variational Autoencoder trained to regress the power transmission, UE association, and PRB allocation decisions, and the second part uses unsupervised learning with a contrastive loss approach to improve the generalization and robustness of the model. We evaluate the performance by comparing its results to those obtained from an exhaustive search and deep Q-network algorithms and reporting performance metrics for the regression task. The results demonstrate the superior efficiency of this approach in different scenarios among the service types, reaffirming its status as a more efficient and effective solution for network slicing problems compared to state-of-the-art methods. This innovative approach not only sets our research apart but also paves the way for exciting future advancements in resource allocation in O-RAN.

Index Terms—Resource allocation, Network slicing, O-RAN, Variational Autoencoder, Contrastive Learning

I. INTRODUCTION

Wireless communication has evolved from a mere convenience to an absolute necessity, driven by an insatiable demand for faster and more dependable connectivity between various quality of service (QoS) requirements [1]. The emergence of fifth generation (5G) technology represents a significant leap, offering the potential to support a wide range of applications, including augmented reality and autonomous vehicles [2]. However, the pursuit of wireless excellence does not conclude with 5G; it marks a stepping stone towards the next frontier—sixth generation (6G), the sixth generation of wireless technology. Poised on the horizon, 6G promises to redefine the boundaries of connectivity again.

Emerging concepts within 6G, such as extreme Multiple-Input Multiple-Output and deep Receiver, promise to propel us further into uncharted technological realms, offering unprecedented data rates and levels of connectivity [3]. These advancements can potentially revolutionize our modes of communication and reshape the fabric of our interconnected world.

Furthermore, the application of various machine learning (ML) techniques to automate resource allocation within the medium access control (MAC) layer and scheduler represents a burgeoning area of research within the 6G landscape [4]. These techniques aim to inject unparalleled intelligence into network management and optimization, laying the foundation for networks capable of dynamically adapting to user demands and environmental conditions. In this constantly evolving landscape, the roles of Open Radio Access Network (O-RAN) [5] and network slicing [6], which have reached remarkable milestones in 5G, continue to be pivotal. As we explore the possibilities offered by 6G and its transformative capabilities, it becomes increasingly clear that the evolution of wireless communication is an ongoing journey, establishing a robust foundation for the next era of wireless excellence.

Resource allocation involves carefully distributing limited network resources among numerous users, applications, or services [7]. In 5G, the main goal is to support a wide range of services, including Enhanced Mobile Broadband (eMBB), Ultra-Reliable Low Latency Communications (URLLC), and massive Machine Type Communications (mMTC) [8]. Each service requires specific resource sets, including bandwidth, data rate, latency, power consumption, complexity, and reliability. Resource allocation within the 5G landscape needs to be flexible to meet these diverse demands while efficiently using network resources.

Network slicing is an innovative concept that customizes virtual networks (slices) within a unified physical infrastructure to address specific service types and use cases [9]. In 5G, it efficiently allocates resources for eMBB and URLLC [10] services. This significance extends into the anticipated 6G era, where network slicing remains instrumental, facilitating resource allocation for diverse applications, including holographic communication and tactile internet [11], [12]. Its inherent scalability ensures adaptability to evolving workloads and user expectations, solidifying its role as a critical technology in the transition from 5G to 6G.

This concept aligns with the architecture of O-RAN. O-RAN is based on open interfaces, open hardware, and open software and aims to provide a more flexible and cost-effective solution for wireless communication [7]. Implementing network slicing in O-RAN optimizes resource allocation and promotes multi-vendor interoperability and innovation.

The core of O-RAN's architecture consists of two funda-

mental components: Radio Units (RUs), responsible for physical layer functions, and Distributed Units (DUs), which manage baseband processing and control. These components work together, with the Central Unit (CU) serving as a centralized coordinator for network resources, facilitating dynamic resource allocation [5], [13]. The CU further comprises two distinct elements: the control plane (CP) and the user plane (UP). Adding to O-RAN's adaptability and innovation are xApps (cross-applications), capable of spanning multiple network domains to optimize resource allocation for various services. These network segments include Fronthaul, Backhaul, and Midhaul, facilitating data transmission between components. Overseeing resource management and orchestration tasks is the Management and Orchestration (MANO) layer, ensuring the network's efficiency. Network Functions Virtualization (NFV) decouples software from hardware, enhancing scalability. Furthermore, the Radio Access Network Intelligent Controller (RIC) plays a pivotal role in intelligent resource control, enabling dynamic allocation to meet diverse service requirements [5]. These components collectively define O-RAN's transformative architecture, promoting openness, adaptability, and efficient resource utilization in modern wireless networks.

It is worth noting that O-RAN comprises two types of RIC: near-real-time (near-RT) RIC, which manages Radio Access Network (RAN) control and optimization, and non-real-time (non-RT) RIC. Within the near-RT RIC, xAPPs facilitate RAN control and optimization, while inside the non-RT RIC, rAPPs support it by providing guidance and employing ML models. Furthermore, both xAPPs and rAPPs can be implemented by third-party entities, allowing for a diverse ecosystem of applications within the O-RAN architecture [14].

Using xAPPs leverages O-RAN network slicing to use resources efficiently and facilitate collaboration across services. However, this also introduces complexities in network management, as each xAPP needs to adjust the different QoS requirements of multiple services, posing a coordination challenge. Furthermore, cellular operators face the difficulty of establishing consistent connectivity for devices with varying QoS demands [15], [16]. Therefore, this study addresses the resource allocation problem within O-RAN using network slicing by considering the xAPPs. We propose a novel resource allocation method to effectively coordinate the numerous independent xAPPs to address network slicing and resource allocation challenges.

The use of ML algorithms in wireless networks has increased due to the growing complexity of these networks and the challenges of creating custom optimization models. Traditional approaches, such as convex/non-convex optimization, are struggling with the increasing complexity stemming from changes in network architecture, evolving performance requirements, and the growing number of devices. Current methods for network resource allocation that rely on learning-based techniques, like deep learning (DL) and deep reinforcement learning (DRL), often overlook the ability to learn resource distributions. Typically, these methods involve designing an agent for a specific task and training it from scratch, which reduces exploration efficiency and extends convergence times. Moreover, they require many training samples, leading

to prolonged exploration phases.

The limited adaptability of traditional ML methods to new scenarios motivates us to explore an alternative approach capable of better generalization, more efficient data utilization, and resource distribution learning. To address these objectives, we propose a novel methodology that uses a self-supervised learning technique, specifically contrastive learning [17], in combination with a variational autoencoder (VAE) model, which is a type of generative model [18]. These models excel in handling uncertainty by learning distributions, offering a distribution for predictions instead of a singular deterministic output.

Moreover, their skill in handling incomplete or missing data allows them to fill in missing values based on learned patterns. VAEs also excel in semi-supervised learning setups, effectively using labeled and unlabeled data to improve predictive accuracy. Their generative abilities enable the creation of new data instances that resemble the training set, which is helpful in scenarios requiring synthetic data generation or increased resilience against noise and outliers.

Furthermore, contrastive learning involves comparing different examples to acquire informative data representations. On the other hand, a VAE consists of an encoder and decoder that work together to learn the underlying probability distribution of data. By integrating contrastive learning with VAE, we can address the challenge of needing many training samples in ML. This approach can improve performance metrics, leading to faster convergence and better results while reducing the time and effort required for algorithm design and training.

In our proposed solution, x-Apps help to implement advanced resource allocation algorithms within the O-RAN framework. The algorithm is deployed as an x-App on the near-real-time RIC, enabling efficient and dynamic resource allocation adjustment based on real-time network conditions and user demands.

A. Contribution

This paper introduces a system model in the O-RAN architecture that provides support for two primary services, namely eMBB and URLLC. It focuses on resource allocation, with a particular emphasis on network slicing. The primary contributions of our paper can be summarized as follows:

- Our research aims to address the resource allocation problem in the O-RAN architecture, explicitly focusing on optimizing weighted throughput by allocating resources such as transmission power and Physical Resource Blocks (PRBs). We consider the unique QoS requirements and service priorities of two key 5G services: eMBB and URLLC. Compared to existing joint resource allocation schemes, our xAPP-based architecture enhances network management flexibility.
- Our approach to optimizing resource allocation involves two main steps. Firstly, we simplify the problem by framing it as an optimization problem. Then, we introduce a novel machine learning algorithm that combines supervised learning with a VAE and unsupervised learning with contrastive loss to optimize resource allocation in

O-RAN. It significantly improves the model’s generalization ability, making it a more practical solution for real-world applications.

- While explicitly guaranteeing a global optimal solution is difficult, our method aims to achieve near-optimal solutions through evaluation with multiple benchmarks and significantly lower computational costs, making it a robust and practical solution for modern O-RAN systems. The method balances computational efficiency and scalability, making it suitable for real-time resource allocation in dynamic O-RAN environments. It is not limited to O-RAN and can be applied to future multi-vendor O-RAN architectures, leveraging semi-supervised generative model principles developed by our team.

B. Structure of Paper

The paper is structured as follows: Section II reviews related works. In Section III, we introduce the system model for the resource allocation problem in the O-RAN architecture and formally define the resource allocation problem as an optimization problem. Section IV provides a detailed description of the proposed resource allocation algorithm. Section V presents numerical results used to evaluate the algorithm’s performance. Section VI compares the computational cost of employed algorithms. Finally, Section VII offers our conclusion.

II. RELATED WORKS

As mentioned in Section I, cellular operators face significant challenges in ensuring reliable connections for devices with diverse QoS requirements. This challenge becomes more prominent in 5G and 6G networks due to their increased complexity and stringent QoS demands [16]. Recently, a growing focus has been on addressing the network slicing problem in cellular networks [16], [19]–[22].

Feng et al. [16] proposed a method that employs network slicing and scheduling to allocate resources based on QoS requirements. Another study presented a resource allocation approach based on the M/M/1 queuing system for RAN slicing [19]. Nevertheless, practical scenarios often involve bursty traffic, overly optimistic, rendering the M/M/1 assumption of a Poisson distribution of packet arrivals at each gNodeB, which serves the eMBB and URLLC services. Consequently, the gNodeB cannot be considered an M/M/1 system, and its queue cannot be accurately modeled as a continuous-time Markov process. Additionally, in a study by Kazemifard et al., [20], an O-RAN system was investigated, assuming that the core network and RAN are co-located in the same data center. The authors conducted a theoretical analysis and employed a mathematical model to address minimum delay problems efficiently.

Various approaches have been proposed in the literature to address resource allocation challenges in wireless networks, including optimization techniques, game theory, and ML algorithms [23]. ML algorithms, in particular, have found application in power control and resource allocation within wireless networks.

For instance, the SAMUS framework was employed by Bektas et al. [24] to forecast incoming traffic, enabling an exploration of various network slicing operations and a discussion of the trade-off between the data rate of eMBB and the latency of URLLC. Li et al. [25] introduced a method that utilizes DRL for proactive resource allocation to mobile UE, considering both time and frequency domains while accounting for mobility. Wu et al. [26] proposed a dynamic resource allocation method for radio and computation resources through RAN slicing, including a defined learning scheme with constraints.

Further, Ayala et al. [27] presented a method for the joint allocation of virtualized RAN’s radio and computation resources using a DRL approach based on an actor-critic network. Wang et al. [28] introduced a DRL-based self-play approach that can be integrated into RAN architecture to efficiently manage RU and DU resources, leading to cost-effective RAN operations. In another approach, Ndikumana et al. [29] combined federated learning and Deep Q-Learning with a reward function to reduce offloading, fronthaul routing, and computation delays in O-RAN.

Similarly, Samarakoon et al. [30] introduced a federated learning algorithm to optimize power transmission and radio resource allocation in vehicular networks. Additionally, Elsayed et al. [31] proposed a reinforcement learning-based method for joint power and radio resource allocation in 5G networks.

III. SYSTEM MODEL AND PROBLEM FORMULATION

In our study, we address the resource allocation problem using network slicing within O-RAN architecture, focusing on two primary slices: the URLLC slice and the eMBB slice. The URLLC slices ensure ultra-low latency and high reliability for critical applications such as autonomous driving and remote surgery. In contrast, eMBB slices focus on high data rates for mobile broadband. Both slices have different QoS requirements for network resource allocation [10].

Slicing the RAN into separate components for URLLC and eMBB optimizes the network for different traffic types and services, improving the efficient and flexible utilization of network resources. Key resources in O-RAN allocation include transmission power and PRBs. Traffic demands, often quantified by data rate and bandwidth, reflect the volume of data requiring transmission through the network. QoS requirements define the desired network performance based on factors such as data rate. The system model for our resource allocation problem with network slicing is illustrated in Fig. 1. Table I describes all variables and parameters used in this study.

In our study, we explore a deployment based on O-RAN, wherein each Base Station (BS), known as RU in O-RAN, supports two different slices: eMBB and URLLC. These slices are designed to meet the QoS requirements of User Equipments (UEs). Our analysis focuses on two key network functions, power control, and radio resource allocation, which are jointly considered. We represent the set of all RUs as \mathcal{B} and the set of UEs as \mathcal{U} . Each BS b serves two sets of UEs: $\mathcal{U}_{e,b}$

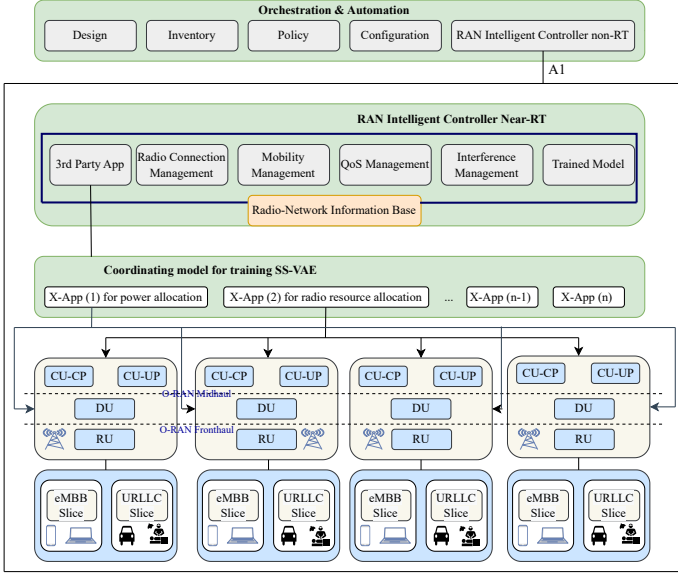


Fig. 1: O-RAN network system model

for eMBB and $U_{u,b}$ for URLLC, leading to a total of U UEs, where $U = U_{e,b} + U_{u,b}$. Each UE is exclusively associated with a single RU. The temporal and spectral layout is divided into \mathcal{M} segments known as PRBs, which are the smallest unit of resources for allocation [32]. Each PRB covers a specific time slot in the temporal domain and a frequency range of f Hz in the spectral domain. We denote S_e for eMBB slices and S_u for URLLC slices. The total number of slices (S) will be $S = S_e + S_u$.

The UE association is indicated by a binary variable $\alpha_{u,b,s}$, which takes a value of 1 if UE u is connected to RU b in slice s , and 0 if not. Since each UE should be connected to only one RU, the following constraint must be met:

$$\sum_{b \in \mathcal{B}} \alpha_{u,b,s} = 1 \quad \forall u \in \mathcal{U}, s \in \mathcal{S}. \quad (1)$$

We define the binary variable $\beta_{u,b,m,s}$ as the indicator for PRB allocation, taking the value of 1 when UE u in slice s is connected to PRB m of RU b , and 0 otherwise.

$$\beta_{u,b,m,s} \leq \alpha_{u,b,s} \quad \forall b \in \mathcal{B}, m \in \mathcal{M}, u \in \mathcal{U}, s \in \mathcal{S}. \quad (2)$$

Similarly, each PRB m of RU b should be associated with only one UE, as defined below:

$$\sum_{u \in \mathcal{U}} \alpha_{u,b,s} \beta_{u,b,m,s} \leq 1 \quad \forall b \in \mathcal{B}, m \in \mathcal{M}, s \in \mathcal{S}. \quad (3)$$

We denote the transmission power of PRB m in RU b in slice s as $p_{u,b,m,s}$ for UE u , and the channel gain between RU b and UE u in slice s as $h_{u,b,m,s}$. The rate achieved for a UE u in slice s by allocating PRB m of RU b is denoted by $R_{u,b,m,s}$, where $\eta_{u,b,m,s}$ represents the Signal to Interference & Noise Ratio (SINR). The calculation for $R_{u,b,m,s}$ is determined by:

$$\eta_{u,b,m,s} = \frac{\alpha_{u,b,s} h_{u,b,m,s} p_{u,b,m,s}}{\sum_{j \neq b}^N \sum_{l \neq s}^S \sum_{i \neq u}^U \alpha_{i,j,l} h_{i,j,m,l} p_{i,j,m,l} + \sigma^2}, \quad (4)$$

$$R_{u,b,m,s} = \log_2(1 + \eta_{u,b,m,s}), \quad (5)$$

$$R_{u,s} = \sum_{b \in \mathcal{B}} \sum_{m \in \mathcal{M}} \alpha_{u,b,s} \beta_{u,b,m,s} R_{u,b,m,s}, \quad (6)$$

$$\begin{aligned} R_u &= \sum_{s \in \mathcal{S}} \sum_{u \in \mathcal{U}} \alpha_{u,b,m,s} \sum_{m \in \mathcal{M}} \beta_{u,b,m,s} R_{u,b,m,s} \\ &= \sum_{u \in \mathcal{U}} \sum_{m \in \mathcal{M}} \beta_{u,b,m} R_{u,b,m,s} \quad \forall m \in \mathcal{M}, s \in \mathcal{S}. \end{aligned} \quad (7)$$

The total power transmitted by RU b and the data rate for UE in the fronthaul link are represented as P_b and C_b , respectively. Quantization noise (σ_1^2) can potentially impact the signal's fidelity during transmission over the fronthaul, mainly when the original signal displays significant variations or spans a wide range of values. This noise may lead to inaccuracies in the transmitted signal, thereby influencing the QoS perceived by the UE. These values are determined as follows:

$$P_b = \sum_{u=1}^U \sum_{m=1}^M \sum_{s=1}^S \alpha_{u,b,s} h_{u,b,m,s} p_{u,b,m,s} + \sigma_1^2, \quad (8)$$

$$\begin{aligned} C_b &= \log_2\left(1 + \frac{\sum_{u=1}^U \sum_{m=1}^M \sum_{s=1}^S \alpha_{u,b,s} h_{u,b,m,s} p_{u,b,m,s}}{\sigma_1^2}\right) \\ &= \log_2\left(\frac{P_b}{\sigma_1^2}\right), \end{aligned} \quad (9)$$

The channel gain matrices in our model are generated using a Rayleigh fading process to simulate variable channel conditions typical in non-line-of-sight environments. The channel vector from the PRB m in RU b to the u UE in the s slice, denoted by $\mathbf{h}_{u,b,m,s}$, is modeled as $\mathbf{h}_{u,b,m,s} = \sqrt{\beta_{u,b,m,s}} \mathbf{g}_{u,b,m,s}$, where $\beta_{u,b,m,s}$ represents the large-scale fading coefficient, accounting for path loss and shadowing, and $\mathbf{g}_{u,b,m,s} \sim \mathcal{N}(0, N_0 I_{D_s})$ is the fast and flat fading effects modeled as a circularly symmetric complex Gaussian random variable. To reflect the impact of interference and uncertainties, the channel gain matrix \mathbf{H} is augmented with Gaussian noise, expressed as $\mathbf{H}_{noise} = \mathbf{H} + \epsilon$, where ϵ is a Gaussian noise matrix with zero mean and adjustable variance σ^2 .

The total delay experienced by each UE is the sum of propagation and transmission delays. The overall propagation delay (D^{pro}) consists of the delays in the fronthaul ($D^{fr,p}$), midhaul ($D^{mid,p}$), and backhaul ($D^{b,p}$) links. In each of these links, the propagation delay is determined as the time it takes for a signal to traverse the distance, calculated as $D = \frac{L}{C}$, where L is the link length and C is the propagation speed. Similarly, the total transmission delay (D^{tr}) is the sum of transmission delays in the fronthaul ($D^{fr,t}$), midhaul ($D^{mid,t}$), and backhaul ($D^{b,t}$) links. Within each link, the transmission delay corresponds to the time needed to transmit all packets into the transmission medium, determined by $D = \frac{\mu}{R_{u,s}}$, where $R_{u,s}$ is the data rate for UE u in slice s , and μ is the mean packet size. The total delay for UE u in slice s is

$D_{u,s} = \frac{L}{C} + \frac{\mu}{R_{u,s}}$, and should be below a specific threshold ($D_{u,s}^{max}$), expressed as $D_{u,s} \leq D_{u,s}^{max}$.

The objective function is designed to optimize the overall network utility, which involves maximizing the weighted sum of the data rates achieved by UEs while ensuring satisfying the QoS requirements. In this context, w_s indicates the priority associated with individual service types. The intelligent RU is responsible for effectively managing the requirements of both network slices. Hence, we can mathematically express the problem in the following manner:

$$\max_{\mathbf{p}, \alpha, \beta} \sum_{s \in \mathcal{S}} \sum_{u \in \mathcal{U}} w_s R_{u,s} \quad (10)$$

subject to

$$P_b \leq P_b^{max} \quad \forall b \in \mathcal{B} \quad (11)$$

$$p_{u,b,m,s} \geq 0 \quad \forall b \in \mathcal{B}, m \in \mathcal{M}, s \in \mathcal{S}, u \in \mathcal{U} \quad (12)$$

$$p_{u,b,m,s} \leq P_s^{max} \quad \forall b \in \mathcal{B}, m \in \mathcal{M}, s \in \mathcal{S}, u \in \mathcal{U} \quad (13)$$

$$R_{u,s} \geq R_s^{min} \quad \forall u \in \mathcal{U}, s \in \mathcal{S} \quad (14)$$

$$C_b \leq C_b^{max} \quad \forall b \in \mathcal{B} \quad (15)$$

$$D_{u,s} \leq D_{u,s}^{max} \quad \forall u \in \mathcal{U}, s \in \mathcal{S}, \quad (16)$$

$$\alpha_{u,b,s} \in \{0, 1\} \quad \forall u \in \mathcal{U}, b \in \mathcal{B}, s \in \mathcal{S} \quad (17)$$

$$\beta_{u,b,m,s} \in \{0, 1\} \quad \forall u \in \mathcal{U}, b \in \mathcal{B}, m \in \mathcal{M}, s \in \mathcal{S} \quad (18)$$

$$\sum_{b \in \mathcal{B}} \alpha_{u,b,s} = 1 \quad \forall u \in \mathcal{U}, s \in \mathcal{S} \quad (19)$$

$$\beta_{u,b,m,s} \leq \alpha_{u,b,s} \quad \forall b \in \mathcal{B}, m \in \mathcal{M}, u \in \mathcal{U}, s \in \mathcal{S} \quad (20)$$

$$\sum_{u \in \mathcal{U}} \alpha_{u,b,s} \beta_{u,b,m,s} \leq 1 \quad \forall b \in \mathcal{B}, m \in \mathcal{M}, s \in \mathcal{S} \quad (21)$$

This formulation can be seen as a well-known NP-hard problem, a multi-dimensional knapsack problem. Since we can reduce it to our resource allocation problem in polynomial time, it follows that it is also NP-hard. Given the NP-hard nature of the resource allocation problem, finding an exact solution in polynomial time is computationally infeasible for large-scale networks.

The system model is constrained by limited resources such as UE or RU and slice power and fronthaul capacity, preventing the aggregate throughput from exceeding its optimal value. This ensures that the objective function, representing aggregate throughput, has an upper bound and cannot increase infinitely. As a result, the algorithm used to solve the system will converge to an optimal solution. If the objective function is a strictly ascending function concerning the number of iterations, it will converge to its global optimum. The algorithm will converge to a local optimum if it is a non-monotonically ascending function. This guarantees the stability and convergence of the system model within the feasible region.

IV. METHODOLOGY

Our research addresses the resource allocation problem within the O-RAN architecture by introducing a semi-

Notation	Definition
b, \mathcal{B}, B	Index, set, and the number of RUs
u, \mathcal{U}, U	Index, set, and the number of UEs
m, \mathcal{M}, M	Index, set, and the number of PRBs per RU
s, \mathcal{S}, S	Index, set, and the number of slices
h, H	Index, and channel gain matrix between RUs and UEs
$\alpha_{u,b,s}$	UE u association to RU b in slice s
$\beta_{u,b,m,s}$	UE u association to PRB m of RU b in slice s
$p_{u,b,m,s}$	Transmission power of PRB m of RU b in slice s
$R_{u,b,m,s}$	Rate achieved for UE u in PRB m of RU b in slice s
$R_{u,s}$	Rate achieved for UE u in slice s
R_u	Rate achieved for UE u
w_s	Priority weights for each service type
P_b	Transmitted power RU in the fronthaul link
C_b	Data rate in the fronthaul link
σ_1^2	Quantization Noise
D^{pro}	Overall propagation delay
$D^{fr,p}$	Propagation delay in the fronthaul link
$D^{mid,p}$	Propagation delay in the midhaul link
$D^{b,p}$	Propagation delay in the backhaul link
L	Length of the fiber link
C	Propagation speed of the medium
D^{tr}	Total transmission delay
$D^{fr,t}$	Transmission delay in the fronthaul link
$D^{mid,t}$	Transmission delay in the midhaul link
$D^{b,t}$	Transmission delay in the backhaul link
R	Data rate of the packet
μ	Mean packet size

TABLE I: Notations with definitions for the system model parameters.

supervised learning algorithm. To achieve this, we have compiled a comprehensive dataset that includes various resource allocation scenarios, covering different objective functions and constraint combinations. We have created labeled data (computed α , β , and transmission powers) using exhaustive search algorithm (ESA), thoroughly exploring the feasible solution space to find the global optimum solution as input for our algorithm's supervised learning part and as a benchmark for models evaluation.

We use a deep neural network (DNN) model with a contrastive loss function to solve the resource allocation problem. This DNN model effectively manages the complexities of resource allocation and acquires the ability to map input features to resource allocation decisions. By training our model, we fine-tune it to estimate resource allocation decisions that fulfill the requirements of the optimization problem (QoS). This semi-supervised learning algorithm, which combines a VAE with a contrastive loss, is denoted as "SS-VAE."

We aim to evaluate the performance of our SS-VAE method using multiple regression-based performance metrics to ensure its robustness. We will also validate the effectiveness of our model by comparing its results with those of the ESA across various scenarios. While ESA is an algorithm for resource allocation decisions that find global optimum solutions, its complexity makes it impractical for real-world deployment. Therefore, we will also compare its performance with state-of-the-art methods known for their practical deployment capabilities, such as DRL. This thorough evaluation will demonstrate the reliability of our method across different scenarios.

Fig. 2 illustrates our proposed methodology for training the SS-VAE and comparing its results with those of the benchmark algorithms.

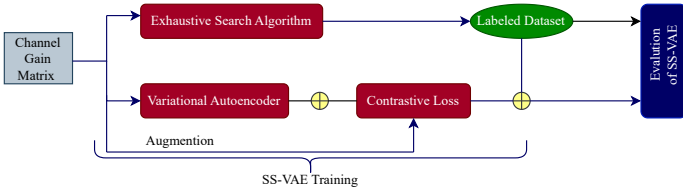


Fig. 2: Overview of the proposed methodology.

A. Exhaustive Search Algorithm

The ESA is a fundamental approach used to find the global optimal solution to resource allocation problems by evaluating all possible configurations and selecting the best one based on a predefined objective function [33]. The ESA is a valuable benchmark solution that provides a ground truth against comparing results from other methods. Its advantages include simplicity of understanding and implementation and the assurance of yielding an optimal solution within a finite time frame. However, its guarantee of optimality comes at the cost of high computational effort, making it suitable primarily for small or well-defined problems where the solution space can be thoroughly explored.

Nonetheless, ESA's main limitation lies in its computational complexity, especially when addressing resource allocation problems with high dimensions and complex constraints. The computational cost increases exponentially as the problem size grows, making ESA impractical for large-scale resource allocation tasks [34]. Despite this limitation, ESA is still widely used as a benchmark for comparing different optimization algorithms and as a reference for evaluating new optimization techniques.

To evaluate the performance, accuracy, and reliability of the SS-VAE method, we will compare its results with those obtained by ESA. We will use the ESA to obtain a subset of solutions for the objective variables (α, β, p) in the resource allocation optimization problem with network slicing. This labeled dataset will be used to train the supervised learning part of our SS-VAE method. The detailed steps of ESA are described in Algorithm 1.

B. Deep Reinforcement learning Algorithm

As discussed in Section II, DRL algorithms effectively address resource allocation, proving their practicality in wireless networks and enhancing key metrics [35]. In this study, we use DRL, where an agent allocates resources based on rewards linked to the objective in Problem 10. Hence, we model the problem as a Markov Decision Process (MDP) and use a DRL algorithm as a benchmark for evaluating our SS-VAE method. In the resource allocation problem (Equation 10), an O-RAN orchestrator is responsible for determining the PRB allocation decisions and identifying the corresponding RU for each UE within each slice. This problem can be represented as a MDP [35]–[38].

- I. **State:** The state at time t ($\mathfrak{s}(t) \in \mathfrak{S}$), is represented by $\{\mathfrak{s}_u(t)\}_{t=1}^N$, where $\mathfrak{s}_u(t)$ indicates the state of UE u ($u = 1 : U$). Here, $\mathfrak{s}_u(t)$ is a binary indicator: it equals

Algorithm 1 ESA for Resource Allocation in O-RAN

Require: $B, U, S, M, w_s, P_b^{max}, P_s^{max}, R_s^{min}, C_b^{max}, D_{u,s}^{min}$, and H

Ensure: Optimal resource allocation $best_solution$ and its objective value $best_value$

- 1: Initialize dataset $\mathcal{X} \leftarrow \emptyset$
 - 2: $best_value \leftarrow -\infty$
 - 3: $best_solution \leftarrow \emptyset$
 - 4: **for** each possible combination of (α, β, p) **do**
 - 5: Calculate $R_{u,s}$ using Eq. (7)
 - 6: **if** all constraints are satisfied **then**
 - 7: $current_value \leftarrow \sum_{s \in S} \sum_{u \in U} w_s R_{u,s}$
 - 8: **if** $current_value > best_value$ **then**
 - 9: $best_value \leftarrow current_value$
 - 10: $best_solution \leftarrow (\alpha, \beta, p)$
 - 11: Add $(\alpha, \beta, p, R_{u,s})$ to dataset \mathcal{X}
 - 12: **end if**
 - 13: **end if**
 - 14: **end for**
 - 15: **return** $best_solution, best_value, \mathcal{X}$
-

one if the data rate requirement of UE u is satisfied and 0 otherwise. Each data rate also corresponds to a quantized transmission power level.

- II. **Action:** An action ($\mathfrak{a} \in \mathfrak{A}$), is represented as $\mathfrak{a} = \{\alpha_{u,b,s}, \{\beta_{u,b,m,s}\}_{m=1}^M\}_{b=1}^B$.
- III. **Transition Probability:** The transition probability $\mathfrak{P}(\mathfrak{s}'|\mathfrak{s}, \mathfrak{a})$ represents the probability of moving from one state \mathfrak{s} to another one \mathfrak{s}' by taking action \mathfrak{a} . It is influenced by several factors, including the QoS requirements of UEs and the resource allocation decisions made for UEs.
- IV. **Reward:** The reward function evaluates the gains or costs of a given state-action pair. It guides the agent's decision-making process by indicating the desirability of various actions across different states. Consistent with previous studies [35]–[37], our approach defines the reward function as a combination of the objective function and the constraints pertinent to the considered problem (Equation 10). Thus, we specify the reward function for our specific scenario as follows:

$$\mathfrak{R}(\mathfrak{s}, \mathfrak{a}) = \Theta_r R_{u,s} + \Theta_{const.} C_{u,b,m,s} + \Theta_{bias}, \quad (22)$$

where, Θ_r , $\Theta_{const.}$, and Θ_{bias} represent the respective weights assigned to the objective function (Data Rate), constraints, and the bias value. The primary objective of the agent is to determine the optimal policy, denoted as $\pi : \mathfrak{S} \rightarrow \mathfrak{P}(\mathfrak{A})$, for the MDP, that maximizes the cumulative reward obtained through dynamic learning from acquired data.

The corresponding value function $V(\pi) : \mathfrak{S} \rightarrow \mathfrak{R}$ is defined as the cumulative discounted reward achieved by following the actions prescribed by the policy π when starting from a specific initial state. Exploring the dynamics of the environment, especially when accounting for variable channel conditions and calculating transition probabilities, is a highly

complex task. Determining the value function in such scenarios presents a significant challenge. Two primary strategies are employed to address MDPs: model-based and model-free approaches. In uncertainty surrounding transition probabilities and reward functions, the model-free approach of Q-learning proves invaluable for solving the MDP [38].

Our resource allocation problem involves managing high-dimensional and complex state and action spaces due to continuous variables like transmission power and numerous UEs and PRB resources. Traditional Q-learning methods struggle in this context because of inefficient learning with rarely encountered state-action pairs [35], [38]. To solve the problem of finding parameters such as transmission power (p), α , and β , we use the Deep Q-Network (DQN) approach, which handles complex state-action spaces by approximating the Q function with a deep neural network. DQN benefits from experience replay and target networks, enhancing learning stability and efficiency [38]. Experience replay stores transition in memory (\mathbb{M}) and samples them to train the neural network ($\mathcal{S}_t, \mathcal{A}_t, \mathcal{R}_t, \mathcal{S}_{t+1}$), reducing correlation in the data and improving gradient estimation. A target network stabilizes learning by updating the Q -network's parameters with independent samples [38].

Our DQN training employs the epsilon-greedy policy for action selection. This means that the agent chooses the action with the highest Q -value with a probability of $1 - \epsilon$, and with a probability of ϵ , it explores and selects a random action. The policy function is represented as:

$$\pi(S) = \begin{cases} \operatorname{argmax}_a Q(\mathcal{S}, a) & \text{with probability } 1 - \epsilon \\ \text{random action} & \text{with probability } \epsilon \end{cases}$$

It is worth noting that the complete training algorithm for DQN is detailed in [38], and for our specific problem, we have utilized Algorithm 3 for training the DQN model.

C. Proposed Method (SS-VAE)

Traditional resource allocation methods in wireless communication systems, such as heuristic and meta-heuristic algorithms, often rely on predefined rules or optimization algorithms that do not adapt well to changing network conditions. In recent times, DL techniques have been used to improve the accuracy and efficiency of resource allocation and transmission power control in wireless communication systems [39]–[42]. These approaches are practical in learning complex, non-linear relationships between input features (e.g., channel matrices) and output decisions (e.g., power and resource allocation).

The distinctive feature of DL-based resource allocation is its capacity to manage wireless communication systems' dynamic and complex nature effectively. DL-based approaches can adjust to changes in network conditions, user demands, and interference patterns, providing more flexible and efficient resource management than traditional methods. Traditional methods often face challenges in real-time adaptation due to predefined rules, complexity in optimization, and a lack of real-time learning. Our SS-VAE method inputs the channel gain matrix into a DNN. This network learns optimal resource

allocation decisions that satisfy network constraints and maximize the weighted aggregated data rate. We use a flattened vector, with dimensions UB , derived from the channel gain matrix as the input for the machine learning model.

Our main contribution involves integrating a VAE with contrastive loss to solve the resource allocation problem. By adding contrastive loss into the VAE's loss function, we enhance the encoder's ability to learn more refined representations, significantly improving the accuracy of resource allocation decisions. The SS-VAE method allows the encoder layers of the VAE to be explicitly utilized for the resource allocation task.

In our problem, the connection between the xApps that handle power transmissions and PRB allocation emerges from their shared foundation within the VAE framework. The VAE operates as a shared space where both xApps come together, enabling a collaborative exploration and consideration of the relevant features for both power transmission and PRB allocations.

The xApps access a common latent representation of the channel gain matrices through this shared space. This shared understanding facilitates a cohesive analysis where the relationships between power transmissions and PRB allocations are thoroughly examined, allowing for the simultaneous consideration of the key features that impact both domains. This integration of information helps make more comprehensive and informed decisions about resource allocation, as it ensures that both xApps use a unified understanding of the underlying data to optimize their respective objectives. This coordination allows for a synchronized approach to resource allocation within the O-RAN architecture.

1) *Variational Autoencoder*: The VAE is a type of DNN generative model used in unsupervised learning tasks. It is designed to generate new data samples that resemble a provided set of training data. One notable advantage of using a VAE is its ability to adeptly capture the intrinsic distribution of the channel gain matrix (input data), which is valuable when addressing the resource allocation problem [43].

In the VAE part of our method, the input data (flattened channel gain matrix) is represented by x , while a lower-dimensional data representation (latent space) is denoted as z . The generative model based on the latent variable is represented as $p_\theta(x)$. The main objective of a VAE is to maximize the likelihood of the data given the model parameters, denoted as θ . This likelihood can be expressed mathematically as:

$$\log p_\theta(x) = \mathbb{E}_{q_\phi(z|x)}[\log p_\theta(x|z)] - D_{KL}(q_\phi(z|x)|p(z)), \quad (23)$$

where $q_\phi(z|x)$ corresponds to the encoder network, which models the posterior distribution of the latent variable based on the input data, the term $D_{KL}(q_\phi(z|x)|p(z))$ represents the Kullback-Leibler (KL) divergence between this posterior distribution and the prior distribution of the latent variable. The loss function (Equation 23) can be optimized by adjusting the parameters of the generative model (θ) and the encoder network represented (ϕ). This optimization process involves iteratively updating these parameters and computing

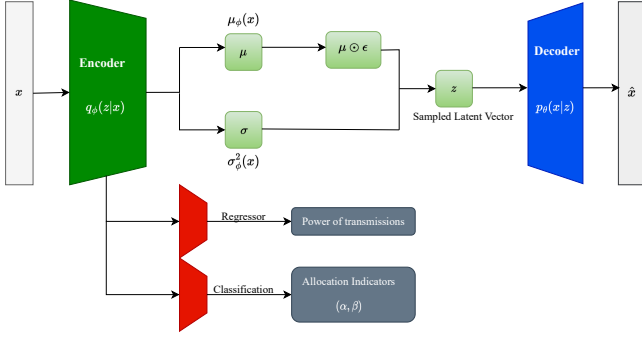


Fig. 3: Architecture of the VAE.

the gradient of the objective with respect to them [43]. The architecture of the VAE for addressing the resource allocation problem with network slicing is illustrated Fig. 3. The VAE comprises an encoder and a decoder. The encoder compresses the channel gain matrix into a lower-dimensional latent code while the decoder reconstructs the channel gain matrix from this code. During training, the VAE minimizes reconstruction loss, improving the accuracy of predicted transmission power.

Several key advantages can be observed when using the VAE for resource allocation. The model can represent complex distributions, capture the non-linear relationship between channel gains and resource allocation decisions, and provide a compressed latent space helpful for visualization, clustering, and anomaly detection tasks. Moreover, resource allocation problems are inherently non-convex and challenging for traditional optimization methods, where the VAEs can propose a more versatile and practical solution to addressing these complexities.

The dataset used to train the SS-VAE model consists of Q training samples, divided into two categories: Q_L labeled samples and Q_U unlabeled samples. These samples are represented by pairs of channel matrices and their corresponding power allocation vectors, denoted as H_i and Γ_i for labeled samples (where i ranges from 1 to Q_L), and H_j for unlabeled samples (where j ranges from 1 to Q_U). The labeled dataset results from the ESA applied to the same training dataset. Specifically, we have used power transmission and allocation decisions (p, α, β) obtained by ESA as labels for training our SS-VAE model.

To train the supervised learning component of our algorithm, we employ the ADAM optimizer [44]. It facilitates the end-to-end training of the VAE using the Q_L labeled samples. The loss function for the regression problem with ADAM optimization is formulated using the mean squared error (MSE) loss function, defined as follows:

$$L_{supervised} = \frac{1}{\beta_L} \sum_{i \in \beta_L} \|\text{encoder}(VAE(H_i)) - \Gamma_i\|^2. \quad (24)$$

The encoder part of the VAE is used to estimate the transmission power and predict the allocation indicators $(\alpha_{u,b,s}$ and $\beta_{u,b,m,s})$. Our model takes a flattened vector of dimension UB as input, obtained from the channel gain matrix.

2) *Contrastive Loss*: Contrastive loss is a widely-used loss function in DL for various representation learning tasks, including image or text classification. Its fundamental aim is to construct a representation of data points that provokes similar data points to be closer together in the representation space while simultaneously pushing dissimilar data points farther apart [17]. Mathematically, the contrastive loss can be expressed as follows:

$$L = \frac{1}{2N} \sum_{i=1}^N (y_i \cdot d^2(\mathbf{x}_i, \mathbf{x}_i^+) + (1 - y_i) \cdot \max(0, m - d^2(\mathbf{x}_i, \mathbf{x}_i^-))), \quad (25)$$

where N is the number of data points, \mathbf{x}_i is the representation of the i^{th} data point, \mathbf{x}_i^+ and \mathbf{x}_i^- are the representations of the similar and dissimilar data points respectively, y_i is a binary label indicating whether \mathbf{x}_i and \mathbf{x}_i^+ are similar or dissimilar, and $d(\mathbf{x}_i, \mathbf{x}_i^+)$ is the distance function between \mathbf{x}_i and \mathbf{x}_i^+ . The parameter m is a margin that separates the similar and dissimilar representations.

To apply contrastive loss in our resource allocation problem, we need to create similar and dissimilar channel gain matrices. This can be achieved using a channel's statistical model that reflects the relevant properties of the communication environment. By introducing randomness through a Rayleigh fading model, we can produce channel gain matrices with varying coefficients in magnitude and phase, thus creating either similar or dissimilar matrices. To generate a channel gain matrix using this approach, we create a matrix of complex Gaussian random variables with zero mean, where the variance is influenced by the distance between the transmitter and receiver while also accounting for interference as noise [45], [46]. The variance can be adjusted to control the level of correlation between the channels, thereby generating similar or dissimilar channel gain matrices as needed. We can train our model with contrastive loss function once we have created similar and dissimilar channel gain matrices. The loss function can be formulated as:

$$L_{Contrastive}(\theta) = \frac{1}{\beta_L} \sum_{i \in \beta_L} \left[-\log \frac{\exp \frac{f(\bar{H}_i)^T \times f(H_i)}{\tau}}{\exp \frac{f(H_i)^T \times f(H_i)}{\tau} + \sum_{i \neq j} \exp \frac{f(H_i)^T \times f(H_j)}{\tau}} \right], \quad (26)$$

where θ is the set of parameters in the VAE model, τ is a temperature hyperparameter, and $L(\theta)$ is the contrastive loss function. \bar{H}_i and \tilde{H}_i are similar matrices to the main channel gain matrix (H_i) and are used in training the SS-VAE model [47]. By minimizing this loss function, we can find a set of parameters that enable our model to differentiate between similar and dissimilar channel gain matrices; therefore, it is used to solve the resource allocation problem.

The connection between the VAE and the additional contrastive loss is essential for an optimal solution. The initial step establishes a strong base by using supervised learning to acquire a good representation of the resource allocation

problem. The subsequent step further improves these representations, enhancing the model's capacity to generalize and effectively handle new, unforeseen scenarios.

3) *Training the SS-VAE model:* The training phase of SS-VAE method consists of two parts. First, supervised learning involves training the VAE and using the VAE's Encoder to predict power transmission. The second part is unsupervised learning, which uses contrastive loss to improve the generalization and robustness of our method.

The latent space dimension represents the size of the hidden representation learned by the VAE [48]. A larger latent space dimension can lead to a more expressive model but also increases the risk of overfitting. The learning rate determines the speed at which the model learns from the data. The batch size determines the number of samples used for each iteration of the training process. The number of epochs determines the number of times the model will be trained on the data. $L1$ and $L2$ regularization to prevent overfitting by adding a penalty term to the loss function of supervised learning [49]. The model is developed using the PyTorch [50] software framework. The dataset's validation and test sizes are 20%, allowing for a more thorough evaluation of the model's performance. Hyperparameter tuning yields the value of hyperparameters, which can be found in Table IV.

4) *Performance Metrics:* The performance metrics for evaluating our approach include Mean Absolute Error (MAE), cosine similarity, and Pearson correlation. MAE, calculated as $MAE = \frac{1}{N} \sum_{i=1}^N |y_i - \hat{y}_i|$, measures the average absolute difference between predicted and actual values. Cosine similarity, given by $Cosine-Similarity(Y, \hat{Y}) = \frac{Y \cdot \hat{Y}}{|Y| |\hat{Y}|}$, assesses the similarity between predicted and actual values in a multi-dimensional space. Pearson correlation, expressed as $correlation(\hat{Y}, Y) = \frac{cov(\hat{Y}, Y)}{\sigma_{\hat{Y}} \sigma_Y}$, represents the variation in the output-dependent attribute that the input-independent variable can predict. In these formulas, N is the total number of samples, y_i and \hat{y}_i represent the true and predicted values, respectively, and the dot product is denoted by \cdot , and vector magnitude by $|\cdot|$. The covariance between predicted and actual values is $cov(\hat{Y}, Y)$, with $\sigma_{\hat{Y}}$ and σ_Y as their standard deviations.

V. SIMULATION RESULTS

We analyzed the initial values in the following subsections to simulate the SS-VAE algorithm. Subsequently, we will compare the results obtained using SS-VAE with those from ESA and DQN.

A. Initial points and performance of training the model

This section presents the numerical results for the resource allocation problem to evaluate the performance of the SS-VAE model compared to ESA and DQN. In our training and testing scenarios, each RU in the O-RAN deployment is equipped with 25 PRBs and operates with a single antenna. We consider a network with two slices, eMBB and URLLC services. These UEs are randomly distributed within a single-cell environment, mostly 200 to 500 meters from the RU. The initial values and parameters used to run and simulate SS-VAE

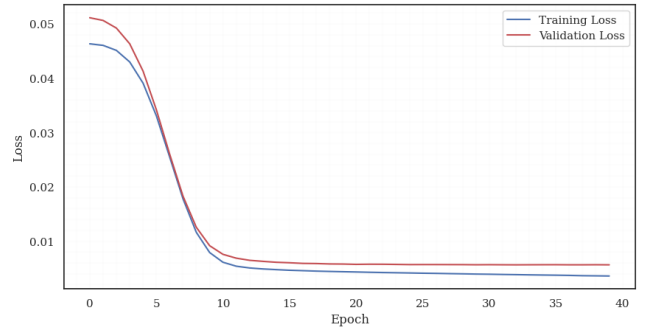


Fig. 4: Loss values of training and validation dataset.

and the benchmark algorithms (ESA and DQN) are provided in Table II, Table III, and Table IV.

Fig. 4 shows the training and validation loss values. The decreasing trend of loss values indicates that the SS-VAE method could accurately estimate the target values (power of transmission, association indicators). The model can map the input channel gain matrix to the power of transmission and the indicators by employing the encoder part of the VAE's to learn the underlying information.

The performance metrics for the test data, as given in Table V, clearly indicate that SS-VAE method obtained optimal performance in the test dataset, demonstrating its generalization ability. The R_{Score}^2 value for the test data indicates that our model successfully explains a significant portion of the variance in estimating the power of transmissions. This improvement can be attributed to the utilization of VAE, which has been proven to enhance generalization in various related tasks. Furthermore, the pre-training method involving contrastive loss has improved our model's ability to learn the underlying features, reducing generalization errors.

B. Comparison of the algorithms

We evaluated the performance of our SS-VAE method compared to the ESA algorithm, focusing on how the number of labeled samples used for training affects the results, as shown in Fig. 5. We analyze the aggregated throughput under varying numbers of labeled data points obtained by SS-VAE algorithm and the ESA. As depicted in Fig. 5a, SS-VAE achieves a similar aggregated throughput compared to the ESA. Moreover, the discrepancy between SS-VAE and the ESA decreases significantly as the number of labeled data points increases. The difference in aggregated throughput between these methods is 2.1 for 2000 labeled samples, which will be decreased using more labeled samples.

We also evaluate the performance of the SS-VAE and ESA based on binary variables related to user association ($\alpha_{u,b,s}$) and PRB allocation ($\beta_{u,b,m,s}$). Fig. 5b displays the ratio of the absolute sum of differences in these binary variables between the SS-VAE and ESA to the total number of them ($\frac{|\alpha_{ESA} - \alpha_{SS-VAE}| + |\beta_{ESA} - \beta_{SS-VAE}|}{\# \text{ Number of } (\alpha \& \beta)}$), as the number of labeled samples increases. The difference between them reaches its minimum at 2000 samples (4.7% error) and is expected to decrease significantly as more labeled samples are used.

TABLE II: Resource Allocation Simulation Parameters

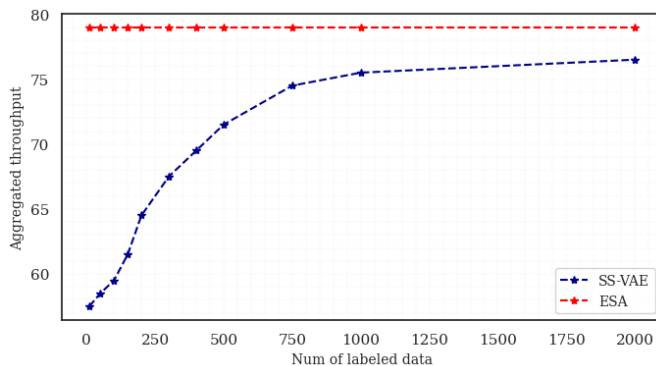
Parameter	Value
Noise power	-174 dBm
bandwidth of each sub-carrier	180 KHz
Maximum transmit power of each O-RU	40 dBm
Maximum fronthaul capacity	46 bps
Maximum data rate for eMBB	20 bps
Maximum data rate for URLLC	2 bps
Maximum power for URLLC & eMBB	30 dBm

TABLE III: DQN Training Parameters

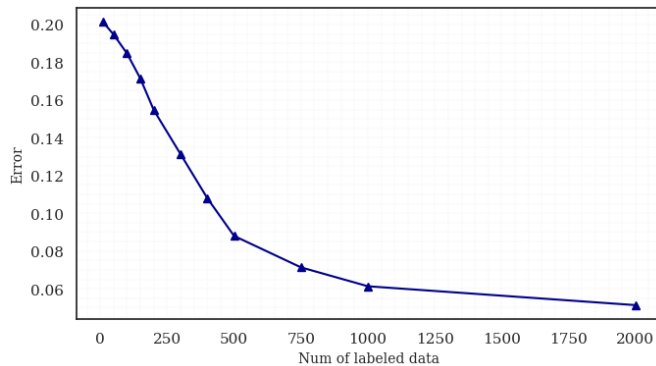
Number of episodes and steps	250, 50
$\gamma, \epsilon_{finalvalue}, \epsilon_{decayfactor}$	0.9, 0.1, 0.9995
Replay memory size	400

TABLE V: Performance metrics of the SS-VAE model

Performance Metric	MAE	R^2_{Score}	Cosine Similarity
Value	0.09207532	0.76795106	0.988023



(a) Aggr. throughput vs. Number of labeled data.



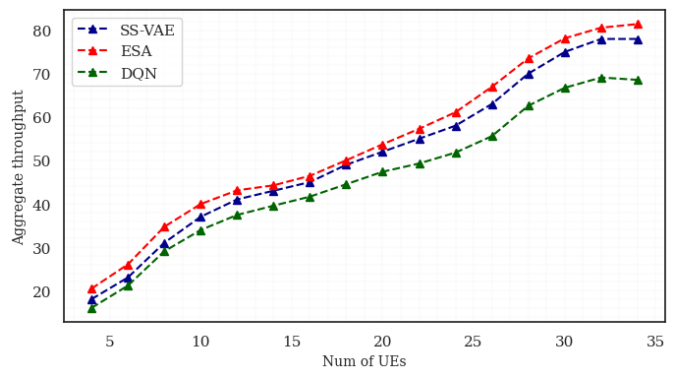
(b) Association Error vs. Number of labeled data.

Fig. 5: Comparison of the algorithms (SS-VAE vs. ESA).

These results demonstrate the reliable performance of our SS-VAE method in addressing the resource allocation problem. The following section will evaluate its performance under varying initial conditions, including different slice numbers, UEs, and transmission power and rate thresholds. Although SS-VAE shows lower error than ESA, it does not perform identically in resource allocation. Therefore, we will also compare it with the DQN algorithm, which has shown effective results in similar resource allocation problems within wireless

TABLE IV: SS-VAE Model Training Parameters

Type	Training Parameter	Value
Optimizer	Initial learning rate	0.001
	β_1	0.99
	β_2	0.99
	Weight Decay	0.9
Model	Number of encoding layer	20
	Dimension of latent space	20
	Contrastive loss temperature	0.25
	Activation Function	ReLU
	Dropout Rate	0.3
Training	Epoch	40
	Batch Size	128
	Train/Validation Split	0.2



(a) Aggr. throughput vs. number of UEs.

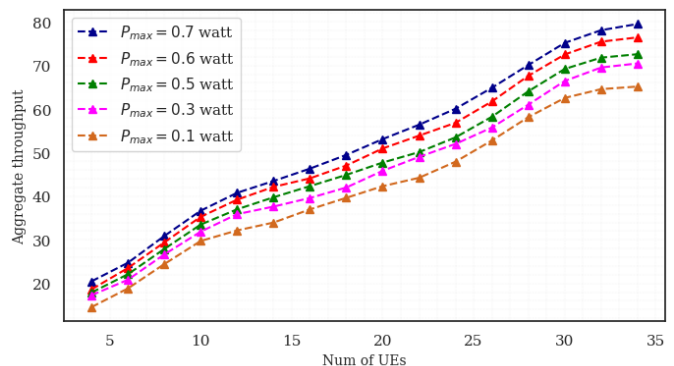
(b) Aggr. throughput vs. number of UEs (P_{O-RU}).

Fig. 6: Aggregated throughput of the SS-VAE vs. Number of UEs.

networks [31], [35], [51].

C. Performance results

Fig. 6 illustrates the aggregate weighted rate across different numbers of UEs as achieved by three algorithms: SS-VAE, ESA, and DQN. Fig. 6a demonstrates the aggregated throughput obtained by SS-VAE, ESA, and DQN for different number of UEs. The difference in performance between SS-VAE and ESA is consistent across all UEs. Moreover, SS-VAE outperforms DQN in aggregated throughput across all UE. In addition, the aggregated throughput increases initially as more UEs join the service for all three examined algorithms.

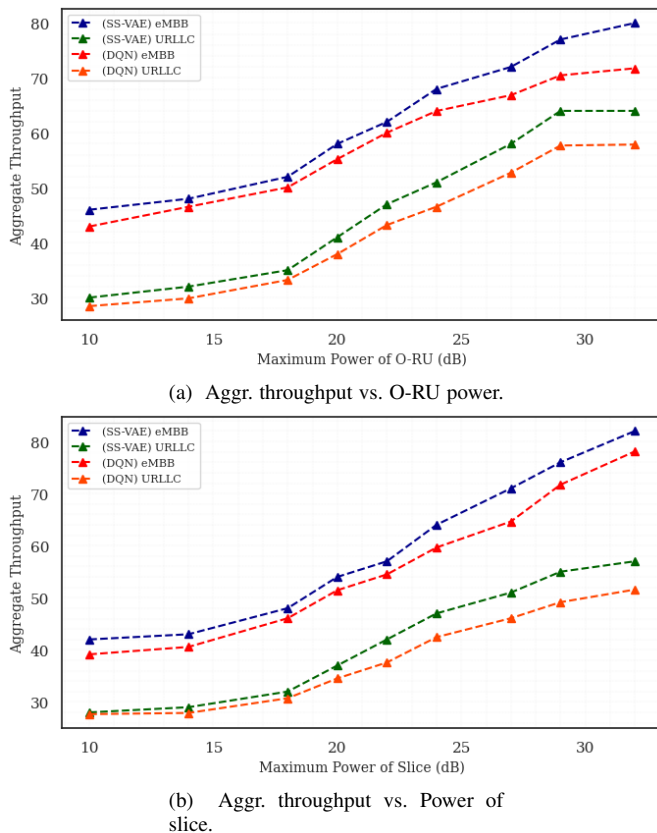


Fig. 7: Aggregated throughput of SS-VAE vs. Power values.

However, it reaches a plateau after 30-35 UEs per service due to power limitations and interference constraints. Fig. 6b shows the aggregated throughput achieved by the SS-VAE algorithm at different maximum power levels of O-RU and different numbers of UEs. In resonance with [15], increasing the maximum power of O-RU and the number of UEs leads to higher aggregated throughput. The highest aggregated throughput is observed when the maximum power of O-RU is at its highest.

Fig. 7 displays the aggregated throughput for two specified service types (eMBB and URLLC), which has been obtained using the SS-VAE and DQN algorithms, about the maximum power of slice and RU. Fig. 7a and Fig. 7b both illustrate the aggregate weighted throughput achieved by SS-VAE and DQN under different maximum power levels for RU and slices, respectively, in eMBB and URLLC services. Both figures demonstrate a direct correlation between increased maximum power levels and higher weighted throughput. Across all scenarios, the SS-VAE algorithm consistently outperforms the DQN algorithm, providing higher aggregate throughput for both service types, regardless of whether the power levels pertain to the RU or the individual slices. Due to their need for higher data rates, eMBB service type exhibits higher aggregate throughput than URLLC services. This consistent performance advantage underscores the effectiveness of the SS-VAE algorithm in optimizing resource allocation across different power settings.

Although ESA ensures a globally optimal solution, its

computational complexity makes it impractical for real-world applications. DQN, while powerful, faces challenges related to convergence time, exploration efficiency, and sample requirements. Our SS-VAE method employs the strengths of supervised and unsupervised learning to provide a scalable and efficient solution for resource allocation in O-RAN, outperforming these benchmarks in real-world scenarios. This contrasts to DQN, which may struggle with generalization due to its reliance on extensive exploration and sample efficiency. Additionally, DQN often requires significant training time to converge to an optimal solution, especially in environments with high variability and complex constraints. It may also face challenges with exploration efficiency, often needing many iterations to fully explore the solution space, resulting in suboptimal performance in dynamic conditions.

VI. COMPUTATIONAL COMPLEXITY ANALYSIS

This section analyzes the computational costs of the ESA, DQN, and the SS-VAE method and discusses how each algorithm scales with increasing network size and complexity.

1) *ESA*: The ESA evaluates all possible combinations of resource allocations to find the global optimal solution. If there are $|U|$ UEs, $|B|$ RUs, M PRBs, and P_{levels} number of discrete power levels, the total cost is given by:

$$\text{Total Cost} = (|U| \times |B|) \times (M + 1)! \times P_{\text{levels}}$$

Where $(M + 1)!$ represents the worst case of assigning UE to PRB or not, ESA needs to scale better with increasing network size and complexity due to its exponential growth in computational requirements. Despite its guarantee of finding the global optimal solution, it is impractical for real-time applications and large-scale networks.

2) *DQN*: The complexity of training a DQN is expressed as $O(E \cdot (T \cdot (|S| \cdot |A| + F)))$, where E is the number of episodes, T is the number of steps per episode, $|S|$ is the size of the state space, $|A|$ is the size of the action space, and F denotes the complexity of the neural network forward pass and backpropagation. The complexity of making a decision using a trained DQN is $O(F)$, where F is the neural network forward pass complexity. The total computational cost for training and inference is dominated by the training phase, which can be expressed as:

$$\text{Total Cost} = O(E \cdot (T \cdot (|S| \cdot |A| + F)))$$

DQN can become computationally expensive as the state and action spaces grow due to the need for extensive exploration and training to converge to an optimal policy. This makes DQN less scalable for large, complex networks.

3) *SS-VAE*: The complexity of training a VAE is $O(E \cdot (D \cdot L + L^2))$, where E is the number of epochs, D is the dimensionality of the input data, and L is the number of latent dimensions. The complexity of inferring resource allocations using a trained VAE is $O(D \cdot L + L^2)$. In addition, the complexity of training with contrastive loss is $O(N \cdot D \cdot L)$, where N is the number of samples. Combining both phases, the total computational cost of the SS-VAE method is:

$$\text{Total Cost} = O(E \cdot (D \cdot L + L^2)) + O(N \cdot D \cdot L)$$

The SS-VAE method scales efficiently with the number of features and samples due to its reliance on learning from

data. While the training phase is computationally intensive, it is performed offline, and the inference phase is relatively lightweight, making it suitable for real-time applications in dynamic O-RAN environments.

4) *Comparison and Implications:* The ESA guarantees finding the global optimal solution, but its computational infeasibility makes it impractical for large-scale networks. DQN provides a scalable solution; however, it requires extensive training and help with efficiency in large, complex networks. The SS-VAE method balances computational efficiency and scalability, making it suitable for real-time resource allocation in dynamic O-RAN environments. It achieves near-optimal performance with significantly lower computational costs, making it a robust and practical solution for modern O-RAN systems.

VII. CONCLUSION

This paper presents a novel model for the downlink of the O-RAN system, designed to coordinate multiple independent xAPPs to address the resource allocation problem with network slicing in the O-RAN architecture. It focuses on optimizing the aggregate weighted throughput by managing RU associations, power allocation, and PRBs to support two central 5G services, eMBB, and URLLC.

Due to the non-convex and NP-hard nature of the resource allocation optimization problem, we proposed a semi-supervised learning approach to solve the resource allocation problem efficiently. Our algorithm begins by reformulating the problem as an optimization problem. The training phase involves supervised learning using a VAE to estimate power transmission and association indicators, followed by unsupervised learning using a contrastive loss approach to improve the model's generalization and robustness.

We compared the SS-VAE method with benchmark algorithms ESA and DQN in various scenarios and discussed their computational complexity. The results indicate that our method performs similarly to ESA while outperforming DQN. We also examined scenarios for eMBB and URLLC services, considering their specific QoS requirements. Through simulations, we demonstrated the efficiency of our model, making it a robust candidate for resource allocation in O-RAN systems. Given the dynamic and complex nature of O-RAN environments, the sample efficiency of our model allows it to adapt to changing conditions without extensive retraining, ensuring high performance with fewer labeled data samples and enabling faster deployment and response times. The SS-VAE model provides robustness, reliability, and generalization from limited data.

In our future research, we aim to explore several areas. Firstly, we intend to evaluate the end-to-end delay experienced by individual UEs and study the impact of deployment costs associated with network function placement. Addressing UE mobility is crucial in practical scenarios. Furthermore, we will explore alternative ML and optimization algorithms to improve our resource allocation approach, paving the way for new research opportunities in this dynamic field.

REFERENCES

- [1] L. M. Larsen, A. Checko, and H. L. Christiansen, "A survey of the functional splits proposed for 5G mobile crosshaul networks," *IEEE Communications Surveys & Tutorials*, vol. 21, no. 1, pp. 146–172, 2018.
- [2] O. Nassef, W. Sun, H. Purmehdi, M. Tatipamula, and T. Mahmoodi, "A survey: Distributed machine learning for 5g and beyond," *Computer Networks*, vol. 207, p. 108820, 2022.
- [3] C.-X. Wang, X. You, X. Gao, X. Zhu, Z. Li, C. Zhang, H. Wang, Y. Huang, Y. Chen, H. Haas *et al.*, "On the road to 6g: Visions, requirements, key technologies and testbeds," *IEEE Communications Surveys & Tutorials*, 2023.
- [4] M. K. Shehzad, L. Rose, M. M. Butt, I. Z. Kovács, M. Assaad, and M. Guizani, "Artificial intelligence for 6g networks: Technology advancement and standardization," *IEEE Vehicular Technology Magazine*, vol. 17, no. 3, pp. 16–25, 2022.
- [5] "O-RAN: Towards an Open and Smart RAN, O-RAN Alliance White Paper, October 2018, O-RAN Alliance."
- [6] S. Zhang, "An overview of network slicing for 5g," *IEEE Wireless Communications*, vol. 26, no. 3, pp. 111–117, 2019.
- [7] A. S. Abdalla, P. S. Upadhyaya, V. K. Shah, and V. Marojevic, "Toward next generation open radio access networks: What o-ran can and cannot do!" *IEEE Network*, vol. 36, no. 6, pp. 206–213, 2022.
- [8] L. Tang, "Multi-dimensional resource allocation algorithm for end-to-end network slicing," 2023.
- [9] A. Oliveira and T. Vazão, "Towards green machine learning for resource allocation in beyond 5g ran slicing," *Computer Networks*, p. 109877, 2023.
- [10] P. Popovski, K. F. Trillingsgaard, O. Simeone, and G. Durisi, "5g wireless network slicing for embb, urllc, and mmcc: A communication-theoretic view," *Ieee Access*, vol. 6, pp. 55 765–55 779, 2018.
- [11] J. Huang, F. Yang, C. Chakraborty, Z. Guo, H. Zhang, L. Zhen, and K. Yu, "Opportunistic capacity based resource allocation for 6g wireless systems with network slicing," *Future Generation Computer Systems*, vol. 140, pp. 390–401, 2023.
- [12] M. Al-Ali and E. Yaacoub, "Resource allocation scheme for embb and urllc coexistence in 6g networks," *Wireless Networks*, pp. 1–20, 2023.
- [13] "Deploying 5G networks, 2020, Nokia corporation. Available at: <https://www.nokia.com/networks/5g/mobile/5g-resources/>."
- [14] L. Bonati, S. D'Oro, M. Polese, S. Basagni, and T. Melodia, "Intelligence and learning in o-ran for data-driven nextg cellular networks," *IEEE Communications Magazine*, vol. 59, no. 10, pp. 21–27, 2021.
- [15] M. K. Motalleb, V. Shah-Mansouri, S. Parsaeefard, and O. L. A. López, "Resource allocation in an open ran system using network slicing," *IEEE Transactions on Network and Service Management*, vol. 20, no. 1, pp. 471–485, 2022.
- [16] L. Feng, Y. Zi, W. Li, F. Zhou, P. Yu, and M. Kadoch, "Dynamic resource allocation with ran slicing and scheduling for urllc and embb hybrid services," *Ieee Access*, vol. 8, pp. 34 538–34 551, 2020.
- [17] T. Chen, S. Kornblith, M. Norouzi, and G. Hinton, "A simple framework for contrastive learning of visual representations," in *International conference on machine learning*. PMLR, 2020, pp. 1597–1607.
- [18] D. P. Kingma and M. Welling, "Auto-encoding variational bayes," *arXiv preprint arXiv:1312.6114*, 2013.
- [19] M. K. Motalleb, V. Shah-Mansouri, and S. N. Naghadeh, "Joint power allocation and network slicing in an open ran system," *arXiv preprint arXiv:1911.01904*, 2019.
- [20] N. Kazemifard and V. Shah-Mansouri, "Minimum delay function placement and resource allocation for open ran (o-ran) 5g networks," *Computer Networks*, vol. 188, p. 107809, 2021.
- [21] J. A. Hurtado Sánchez, K. Casilimas, and O. M. Caicedo Rendon, "Deep reinforcement learning for resource management on network slicing: A survey," *Sensors*, vol. 22, no. 8, p. 3031, 2022.
- [22] B. Adhikari, M. Jaseemuddin, and A. Anpalagan, "Resource allocation for co-existence of embb and urllc services in 6g wireless networks: A survey," *IEEE Access*, 2023.
- [23] Y. Azimi, S. Yousefi, H. Kalbhani, and T. Kunz, "Applications of machine learning in resource management for ran-slicing in 5g and beyond networks: A survey," *IEEE Access*, vol. 10, pp. 106 581–106 612, 2022.
- [24] C. Bektas, D. Overbeck, and C. Wietfeld, "Samus: Slice-aware machine learning-based ultra-reliable scheduling," in *ICC 2021-IEEE International Conference on Communications*. IEEE, 2021, pp. 1–6.
- [25] J. Li, X. Zhang, J. Zhang, J. Wu, Q. Sun, and Y. Xie, "Deep reinforcement learning-based mobility-aware robust proactive resource

- allocation in heterogeneous networks,” *IEEE Transactions on Cognitive Communications and Networking*, vol. 6, no. 1, pp. 408–421, 2019.
- [26] W. Wu, N. Chen, C. Zhou, M. Li, X. Shen, W. Zhuang, and X. Li, “Dynamic ran slicing for service-oriented vehicular networks via constrained learning,” *IEEE Journal on Selected Areas in Communications*, vol. 39, no. 7, pp. 2076–2089, 2020.
- [27] J. A. Ayala-Romero, A. Garcia-Saavedra, M. Gramaglia, X. Costa-Perez, A. Banchs, and J. J. Alcaraz, “vrain: Deep learning based orchestration for computing and radio resources in vrans,” *IEEE Transactions on Mobile Computing*, vol. 21, no. 7, pp. 2652–2670, 2020.
- [28] X. Wang, J. D. Thomas, R. J. Piechocki, S. Kapoor, R. Santos-Rodríguez, and A. Parekh, “Self-play learning strategies for resource assignment in open-ran networks,” *Computer Networks*, vol. 206, p. 108682, 2022.
- [29] A. Ndikumana, K. K. Nguyen, and M. Cheriet, “Federated learning assisted deep q-learning for joint task offloading and fronthaul segment routing in open ran,” *IEEE Transactions on Network and Service Management*, 2023.
- [30] S. Samarakoon, M. Bennis, W. Saad, and M. Debbah, “Federated learning for ultra-reliable low-latency v2v communications,” in *2018 IEEE global communications conference (GLOBECOM)*. IEEE, 2018, pp. 1–7.
- [31] M. Elsayed and M. Erol-Kantarci, “Reinforcement learning-based joint power and resource allocation for urllc in 5g,” in *2019 IEEE Global Communications Conference (GLOBECOM)*. IEEE, 2019, pp. 1–6.
- [32] T. Erpek, A. Abdelhadi, and T. C. Clancy, “An optimal application-aware resource block scheduling in lte,” in *2015 International Conference on Computing, Networking and Communications (ICNC)*. IEEE, 2015, pp. 275–279.
- [33] H. Eiselt, C.-L. Sandblom *et al.*, *Nonlinear optimization*. Springer, 2019.
- [34] J. Nocedal and S. J. Wright, *Numerical optimization*. Springer, 1999.
- [35] A. Filali, B. Nour, S. Cherkaoui, and A. Kobbane, “Communication and computation o-ran resource slicing for urllc services using deep reinforcement learning,” *IEEE Communications Standards Magazine*, vol. 7, no. 1, pp. 66–73, 2023.
- [36] A. Feriani and E. Hossain, “Single and multi-agent deep reinforcement learning for ai-enabled wireless networks: A tutorial,” *IEEE Communications Surveys & Tutorials*, vol. 23, no. 2, pp. 1226–1252, 2021.
- [37] K. Suh, S. Kim, Y. Ahn, S. Kim, H. Ju, and B. Shim, “Deep reinforcement learning-based network slicing for beyond 5g,” *IEEE Access*, vol. 10, pp. 7384–7395, 2022.
- [38] J. Fan, Z. Wang, Y. Xie, and Z. Yang, “A theoretical analysis of deep q-learning,” in *Learning for dynamics and control*. PMLR, 2020, pp. 486–489.
- [39] V. Lima, M. Eisen, K. Gatsis, and A. Ribeiro, “Resource allocation in large-scale wireless control systems with graph neural networks,” *IFAC-PapersOnLine*, vol. 53, no. 2, pp. 2634–2641, 2020.
- [40] P. E. Iturria-Rivera, H. Zhang, H. Zhou, S. Mollahasani, and M. Erol-Kantarci, “Multi-agent team learning in virtualized open radio access networks (o-ran),” *Sensors*, vol. 22, no. 14, p. 5375, 2022.
- [41] N. Hammami and K. K. Nguyen, “On-policy vs. off-policy deep reinforcement learning for resource allocation in open radio access network,” in *2022 IEEE Wireless Communications and Networking Conference (WCNC)*. IEEE, 2022, pp. 1461–1466.
- [42] Q. Wang, Y. Liu, Y. Wang, X. Xiong, J. Zong, J. Wang, and P. Chen, “Resource allocation based on radio intelligence controller for open ran towards 6g,” *IEEE Access*, 2023.
- [43] D. P. Kingma, M. Welling *et al.*, “An introduction to variational autoencoders,” *Foundations and Trends® in Machine Learning*, vol. 12, no. 4, pp. 307–392, 2019.
- [44] D. P. Kingma and J. Ba, “Adam: A method for stochastic optimization,” *arXiv preprint arXiv:1412.6980*, 2014.
- [45] C. Geng, N. Naderializadeh, A. S. Avestimehr, and S. A. Jafar, “On the optimality of treating interference as noise,” *IEEE Transactions on Information Theory*, vol. 61, no. 4, pp. 1753–1767, 2015.
- [46] N. Naderializadeh and A. S. Avestimehr, “Itlinq: A new approach for spectrum sharing in device-to-device communication systems,” *IEEE journal on selected areas in communications*, vol. 32, no. 6, pp. 1139–1151, 2014.
- [47] N. Naderializadeh, “Contrastive self-supervised learning for wireless power control,” in *ICASSP 2021-2021 IEEE International Conference on Acoustics, Speech and Signal Processing (ICASSP)*. IEEE, 2021, pp. 4965–4969.
- [48] Q. Shi, M. Razaviyayn, Z.-Q. Luo, and C. He, “An iteratively weighted mmse approach to distributed sum-utility maximization for a mimo interfering broadcast channel,” *IEEE Transactions on Signal Processing*, vol. 59, no. 9, pp. 4331–4340, 2011.
- [49] K. Janocha and W. M. Czarnecki, “On loss functions for deep neural networks in classification,” *arXiv preprint arXiv:1702.05659*, 2017.
- [50] A. Paszke, S. Gross, F. Massa, A. Lerer, J. Bradbury, G. Chanan, T. Killeen, Z. Lin, N. Gimelshein, L. Antiga *et al.*, “Pytorch: An imperative style, high-performance deep learning library,” *Advances in neural information processing systems*, vol. 32, 2019.
- [51] R. Joda, T. Pamuklu, P. E. Iturria-Rivera, and M. Erol-Kantarci, “Deep reinforcement learning-based joint user association and cu-du placement in o-ran,” *IEEE Transactions on Network and Service Management*, vol. 19, no. 4, pp. 4097–4110, 2022.